Energy Conversion and Management 90 (2015) 128–137

Contents lists available at ScienceDirect

Energy Conversion and Management

journal homepage: www.elsevier.com/locate/enconman

Nonlinear modeling and dynamic analysis of hydro-turbine governing system in the process of load rejection transient

Hao Zhang, Diyi Chen *, Beibei Xu, Feifei Wang

Institute of Water Resources and Hydropower Research, Northwest A&F University, Yangling, Shaanxi 712100, PR China

ARTICLE INFO

Article history:
Received 22 August 2014
Accepted 8 November 2014

Keywords:
Hydro-turbine governing system
Dynamic transfer coefficients
Nonlinear dynamics
Mathematical modeling

ABSTRACT

This article pays attention to the mathematical modeling of a hydro-turbine governing system in the process of load rejection transient. As a pioneer work, the nonlinear dynamic transfer coefficients are introduced in a penstock system. Considering a generator system, a turbine system and a governor system, we present a novel nonlinear dynamical model of a hydro-turbine governing system. Fortunately, for the unchanged of PID parameters, we acquire the stable regions of the governing system in the process of load rejection transient by numerical simulations. Moreover, the nonlinear dynamic behaviors of the governing system are illustrated by bifurcation diagrams, Poincare maps, time waveforms and phase orbits. More importantly, these methods and analytic results will present theoretical groundwork for allowing a hydropower station in the process of load rejection transient.

1. Introduction

With the development of hydroelectric power industry, special attentions need to be paid to ensure the stability and safety of water turbine generator in the process of operation [1–6]. As we all know, hydraulic turbine governing system (HTGS) is one of the most important parts of hydropower plant, which plays a key role in maintaining safety, stability and economical operation for the hydropower plant [7–14]. Therefore, the study of the governing system becomes a necessary and important issue.

Transition process makes up of two phases: large fluctuation process and small fluctuation process. Most published papers have focused on the modeling of hydro-turbine governing system in the process of small fluctuation and not suitable to describe large fluctuation process [15–25]. However, turbine characteristic is very complex with violent changes of parameters in the process of large fluctuation. Therefore, the research of hydro-turbine needs attention in the process of large fluctuation.

Motivated by the above discussions, we have three advantages which make our approach attractive comparing with the prior works. Firstly, a novel nonlinear dynamic mathematic model of a hydro-turbine-generator unit system is established, which is more accordance with the actual project. Secondly, as a pioneering work, nonlinear dynamic transfer coefficients are introduced to the above system. Thirdly, the nonlinear dynamical behaviors of the above system with six nonlinear dynamic transfer coefficients are studied in detail.

The rest of the paper is organized as follows: in Section 2, a novel nonlinear dynamic mathematical model of a hydro-turbine-generator unit is established. Section 3 analyzes the nonlinear dynamical behaviors of the presented system in the process of load rejection transient. Section 4 closes the paper.

2. Mathematical model of hydro-turbine governing system

2.1. Linear mathematic model

The structure of Francis turbine unit governing system is shown in Fig. 1.

For Francis turbine, the dynamic characteristics [26–30] can be described as

$$\begin{cases} M_t = M_t(H, n, a) \\ Q = Q(H, n, a) \end{cases}, \tag{1}$$

where the M_t, Q, H, n and a denote the mechanical torque of turbine, turbine flow, turbine head, rotate speed and guide vane opening, respectively. The corresponding relative deviation are m_t, q, h, x and y, respectively. Considering the guide vane opening a has an asymptotically linear relationship with main servomotor stroke y, we replace a with y and acquire the dynamic characteristics expression of hydro-turbine.

$$\begin{cases} m_t = e_{mw}x + e_{my}y + e_{mh}h \\ q = e_{qw}x + e_{qy}y + e_{qh}h \end{cases}, \tag{2}$$

* Corresponding author. Tel.: +86 181 6198 0277.
E-mail address: diyichen@nwsuaf.edu.cn (D. Chen).

http://dx.doi.org/10.1016/j.enconman.2014.11.020
0196-8904/

Nomenclature

M_t	mechanical torque of the turbine, N m	β_0	runner intermediate flow surface angle, rad
H	turbine head, m	α	guide vane discharge angle, rad
N	turbine/rotor speed, rad/s	b_0	guide vane height, m
A	guide vane opening, m	F	runner outlet area, m^2
Q	turbine flow, m^3/s	r_0	runner intermediate flow surface radius, m
m_t	turbine torque relative deviation, p.u.	D_0	guide vane pitch circle diameter, m
q	incremental turbine flow deviation, p.u.	L	guide vane width, m
x	incremental turbine speed deviation, p.u.	Z_0	number of guide vane
y	incremental guide vane/wicket gate position deviation, p.u.	Y	guide vane angle, rad
		D_1	runner diameter of hydro-turbine, m
h	incremental turbine head deviation, p.u.	e_{mx}, e_{my}, e_{mh}	partial derivatives of the hydro-turbine torque with respect to head, guide vane and turbine speed, p.u.
T_w	water starting time, s		
T_{ab}	mechanical starting time, s	e_{qx}, e_{qy}, e_{qh}	partial derivatives of the flow with respect to head, guide vane and turbine speed, p.u.
T_y	engager relay time constant, s		
m_{g0}	load torque disturbance	e_n	synthetic self-regulation coefficient
r	frequency disturbance	k_p	proportional adjustment coefficient
u	regulator output	k_i	integral adjustment coefficient
z	intermediate variable	k_d	differential adjustment coefficient
β	normal angle of guide vane, rad		

where $e_{mw} = \frac{\partial m_t}{\partial x}$, $e_{my} = \frac{\partial m_t}{\partial y}$ and $e_{mh} = \frac{\partial m_t}{\partial h}$ denote partial derivatives of the hydro-turbine torque with respect to head, guide vane and turbine speed, respectively. $e_{qw} = \frac{\partial q}{\partial x}$, $e_{qy} = \frac{\partial q}{\partial y}$ and $e_{qh} = \frac{\partial q}{\partial h}$ denote partial derivatives of the flow with respect to head, guide vane and turbine speed, respectively.

2.2. The dynamic characteristics of penstock system

When the elasticity of water and tube wall shows no significant effects on the water hammer, we consider it as rigid water

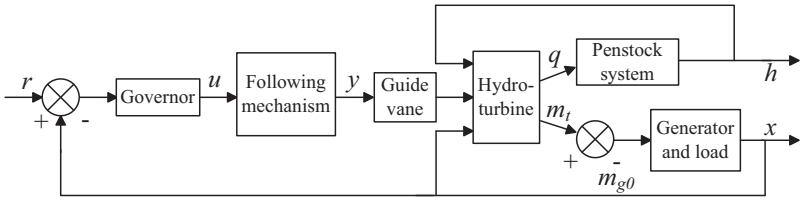

Fig. 1. Governing system structure diagram of Francis turbine unit.

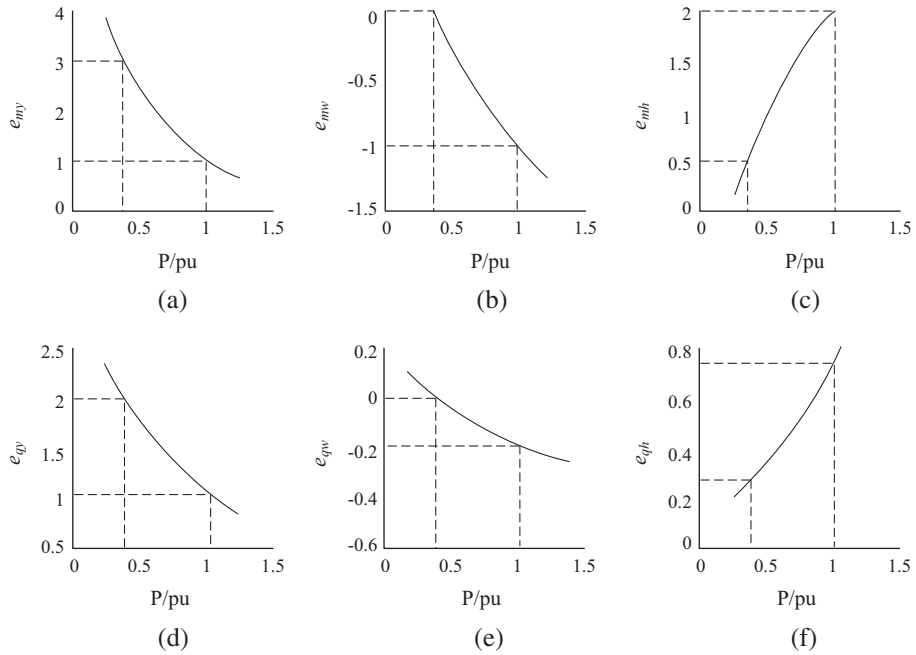

Fig. 2. Curves of hydro-turbine transfer coefficient.

hammer. And the dynamic characteristics of the penstock system can be described as

$$h = -T_w \frac{dq}{dt}, \tag{3}$$

where T_w denotes the water inertia time constant of the pressure diversion system.

2.3. The dynamic characteristics of generator and load

$$T_{ab}\frac{dx}{dt} + e_n x = m_t - m_{g0}, \tag{4}$$

where T_a, T_b denote the inertia time constant of generator and load, respectively, $T_{ab} = T_a + T_b$. e_n is the synthetic self-regulation coefficient.

2.4. The dynamic characteristics of hydraulic servo system

$$T_y \frac{dy}{dt} + y = u, \tag{5}$$

where T_y, u denote the engager relay time constant and regulator output, respectively.

From Eqs. (2) and (3), we can get

$$\frac{dh}{dt} = \frac{e_{qx}e_n}{e_{qh}T_{ab}}x + \frac{e_{qy}T_{ab} - e_{my}e_{qx}T_y}{e_{qh}T_yT_{ab}}y - \frac{T_{ab} + e_{qx}e_{mh}T_w}{e_{qh}T_wT_{ab}}h - \frac{e_{qy}}{e_{qh}T_y}u + \frac{e_{qx}}{e_{qh}T_{ab}}m_{g0}. \tag{6}$$

From the above equations, we can get the linear first-order differential equation system of hydro-turbine governing system as

$$\begin{cases} \dot{x} = -\frac{e_{mw}-e_n}{T_{ab}}x + \frac{e_{my}}{T_{ab}}y + \frac{e_{mh}}{T_{ab}}h - \frac{1}{T_{ab}}m_{g0} \\ \dot{y} = \frac{1}{T_y}(u - y) \\ \dot{h} = \frac{e_n e_{qw}}{e_{qh}T_{ab}}x + \left(\frac{e_{qy}}{e_{qh}T_y} - \frac{e_{qw}e_y}{e_{qh}T_{ab}}\right)y - \left(\frac{e_{qw}e_h}{e_{qh}T_{ab}} + \frac{1}{e_{qh}T_w}\right)h - \frac{e_{qy}}{e_{qh}T_y}u + \frac{e_{qw}}{e_{qh}T_{ab}}m_{g0} \end{cases}. \tag{7}$$

2.5. The nonlinear dynamic expression of hydro-turbine transfer coefficients

Currently, there are three ways to calculate the transfer coefficients of hydro-turbine which include external characteristics [26], internal characteristics [31] and simple analytical method [32,33]. In this article, we consider Francis turbine governing system as the subject. By utilizing the internal characteristics, we acquire the non-linear relationship between time t and the transfer coefficients in the process of load rejection transient.

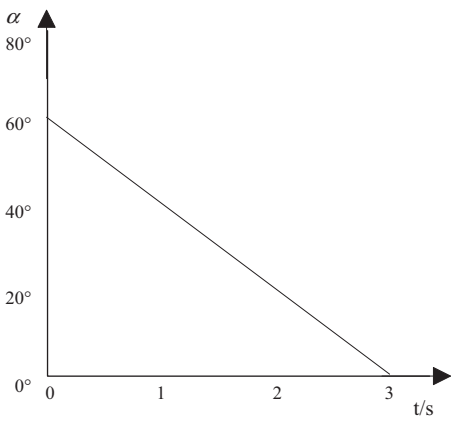

Fig. 3. The closing rule of guide vane in the process of load rejection transient.

The steady state equation of Francis turbine [31] can be shown as

$$Q = \left(\frac{nr_0^2 + \frac{9.8\eta H}{n}}{\frac{ctg\alpha}{2\pi b_0} + r_0\frac{ctg\beta_0}{F}}\right), \tag{8}$$

and

$$M_t = Q\left[\left(\frac{ctg\alpha}{2\pi b_0} + r_0\frac{ctg\beta_0}{F}\right)Q - nr_0^2\right], \tag{9}$$

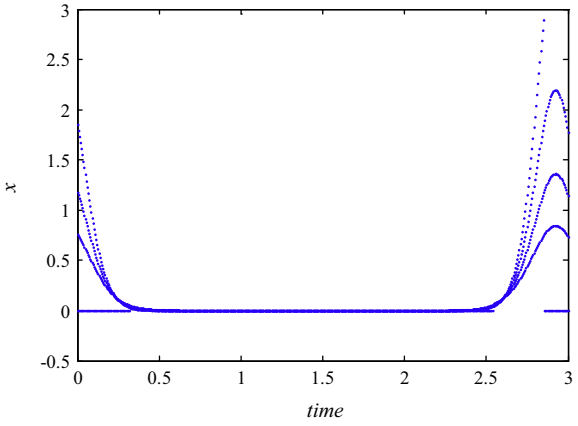

(a) Bifurcation diagram of Eq. (25) with $(0 \le t \le 3)$

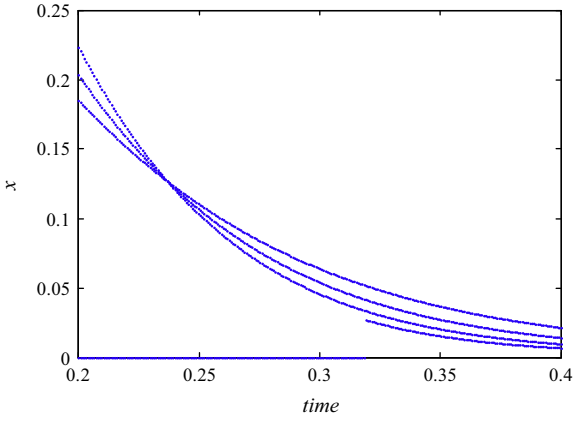

(b) Local amplification of the bifurcation diagram with $(0.2 \le t \le 0.4)$

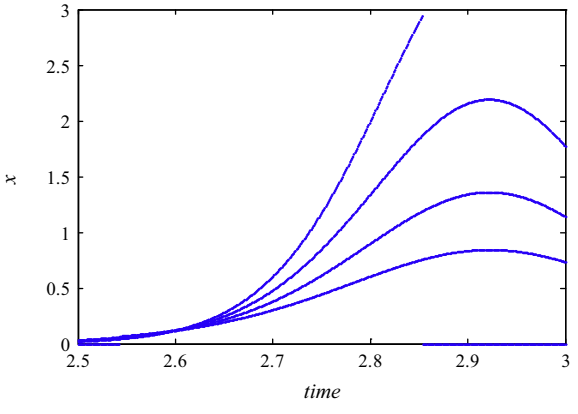

(c) Local amplification of the bifurcation diagram with $(2.5 \le t \le 3)$

Fig. 4. Bifurcation diagram of Eq. (25) with the differential adjustment coefficient t.

where H, M_t, n, Q, α are parameters of operation. They are turbine head, torque of turbine, rotor velocity, turbine flow, guide vane angle, respectively. b_0, F, r_0, β_0 are guide vane height, runner outlet area, runner intermediate flow surface radius, runner intermediate flow surface angle.

We standardize Eqs. (8) and (9), and the transfer coefficients formulas of turbine internal characteristics can be obtained as

$$e_{qy} = \frac{a_0}{1 + a_0 - c_0} \cdot \frac{q_0^2 \csc^2 \alpha_0}{\omega_0} \cdot \frac{Y_R Q_R}{2\pi b_0 r_0^2 k_0 \omega_R}, \tag{10}$$

$$e_{qw} = \frac{a_0 - 1}{1 + a_0 - c_0} \cdot \frac{q_0}{\omega_0}, \tag{11}$$

$$e_{qh} = \frac{1}{1 + a_0 - c_0} \cdot \frac{q_0}{h_0}, \tag{12}$$

$$e_{my} = b e_{qy}, \tag{13}$$

$$e_{mw} = b e_{qw} - \frac{m_{t0}}{\omega_0}, \tag{14}$$

$$e_{mh} = b e_{qh} + \frac{m_{t0}}{h_0}, \tag{15}$$

where $a_0 = \frac{\omega^2}{\eta h} \cdot \frac{r_0^2 \omega_R^2}{9.81 H_R}$, $b = (1 + c)\frac{m_t}{q}$, $r_0 = 0.353 D_1$, $c_0 = \frac{2q_0(q - q_*)Q_R^2}{2d\eta_0 - (q_0 - q_*)^2 Q_R^2}$, $k_0 = \left(\frac{dy}{d\alpha}\right)$. d is constant of flow passage component, D_1 is runner

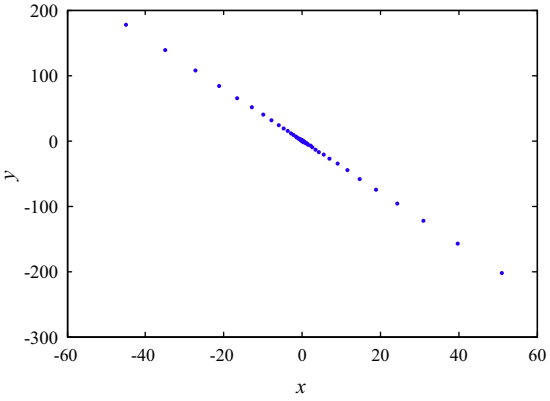

(a) Poincare map

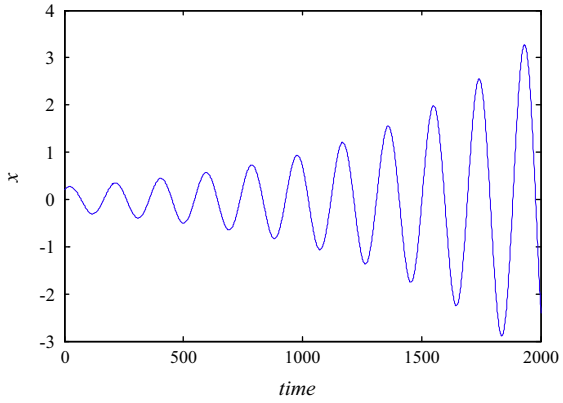

(b) time waveforms with x-t

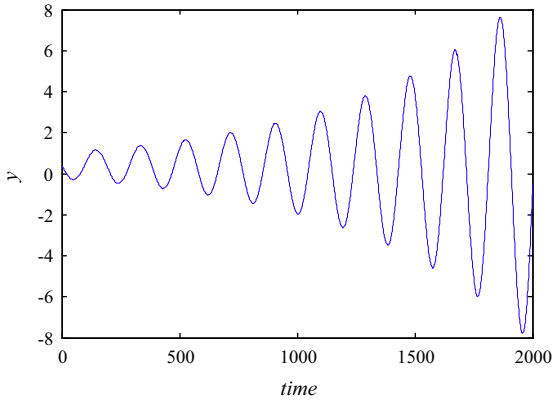

(c) time waveforms with y-t

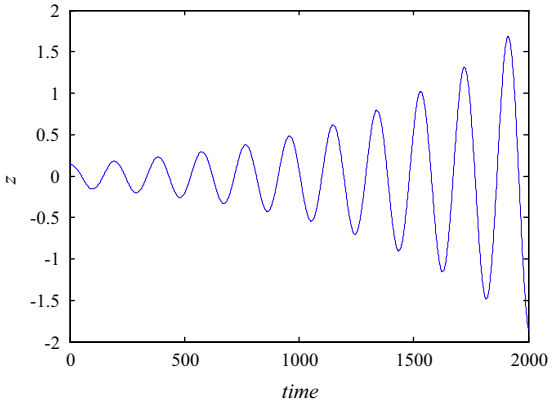

(d) time waveforms with z-t

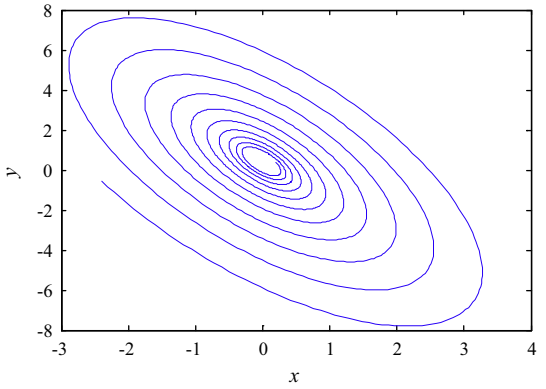

(e) phase orbit with x-y

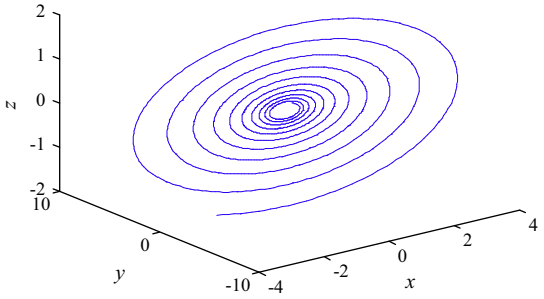

(f) phase orbit with x-y-z

Fig. 5. Poincare maps, time waveforms and phase orbits with $t = 0.1$.

diameter of turbine, subscript $*$, R denotes the most excellent operating mode and actual value of rated condition, respectively.

In order to get k_0 in Eq. (10), the relationship between guide vane angle Y and guide vane discharge angle α, can be written as

$$Y = D_0 \sin\left(\frac{\beta}{2}\right) \sin\left(\alpha + \frac{\beta}{2}\right) - L \sin\left(\frac{\beta}{2}\right), \tag{16}$$

where D_0 is guide vane pitch circle diameter, L is guide vane width, β and Z_0 are normal angle and number of guide vane, respectively.

We use the approximate relationship between turbine flow and turbine efficiency to acquire c, and the approximate relations can be written as

$$\eta = \eta_* - \frac{(q - q_*)^2 Q_R^2}{2d}. \tag{17}$$

The method of internal characteristics calculate is used to get the relation curve between transfer coefficients and power of hydro-turbine (HL240-LJ-140). And the basic hydro-turbine parameters as follows

$D_1 = 1.4$ m, $b_0 = 0.511$ m, $Z_0 = 16$, $D_0 = 1.6$ m, $P_R = 3376$ kw, $a_R = 0.137$ m.

The relation curves are shown in Fig. 2.

The closing time of guide vane is set for 3 s, and the closing rule can be shown in Fig. 3.

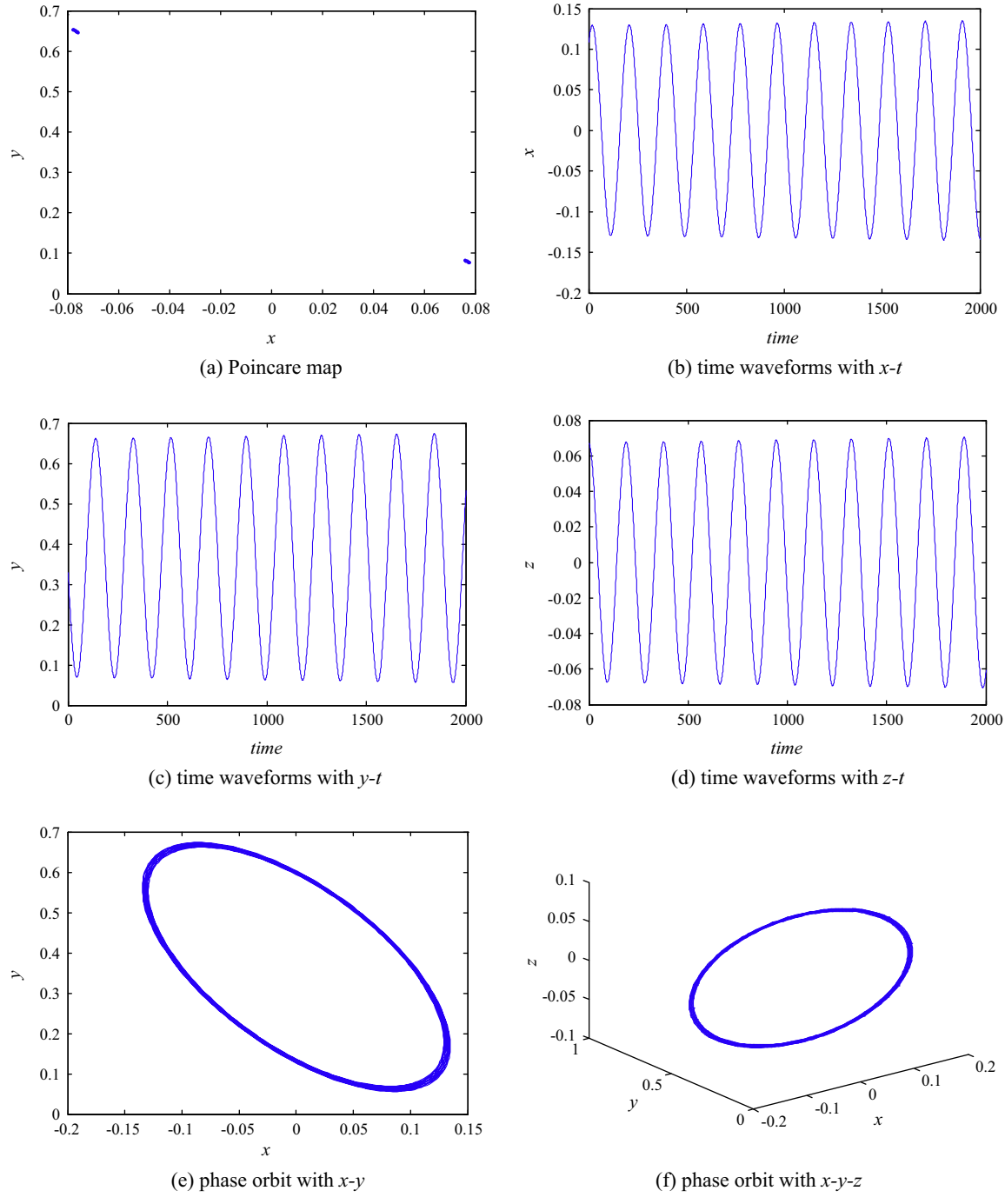

(a) Poincare map

(b) time waveforms with x-t

(c) time waveforms with y-t

(d) time waveforms with z-t

(e) phase orbit with x-y

(f) phase orbit with x-y-z

Fig. 6. Poincare maps, time waveforms and phase orbits with $t = 0.22$.

According to the above analyses, in the process of load rejection transient, we suppose that the change value of transfer coefficients are in the range of the curves (Fig. 2). The correlation of turbine flow, turbine speed and efficiency is analyzed, which influences the values of transfer coefficients. Based on this, the nonlinear expressions between transfer coefficients and time t are obtained by introducing trigonometric function, and the equations can be written as

$$e_{my} = \cos\left(\frac{2}{3}\pi t + \pi\right) + 2, \tag{18}$$

$$e_{mw} = \frac{1}{2}\cos\left(\frac{2}{3}\pi t + \pi\right) - \frac{1}{2}, \tag{19}$$

$$e_{mh} = \cos\left(\frac{2}{3}\pi t + \frac{1}{3}\pi\right) + 1, \tag{20}$$

$$e_{qy} = \frac{1}{2}\sin\left(\frac{2}{3}\pi t - \frac{1}{2}\pi\right) + \frac{3}{2}, \tag{21}$$

$$e_{qw} = \frac{1}{10}\sin\left(\frac{2}{3}\pi t - \frac{\pi}{2}\right) - \frac{1}{10}, \tag{22}$$

$$e_{qh} = \frac{1}{4}\sin\left(\frac{2}{3}\pi t + \pi\right) + \frac{1}{2}. \tag{23}$$

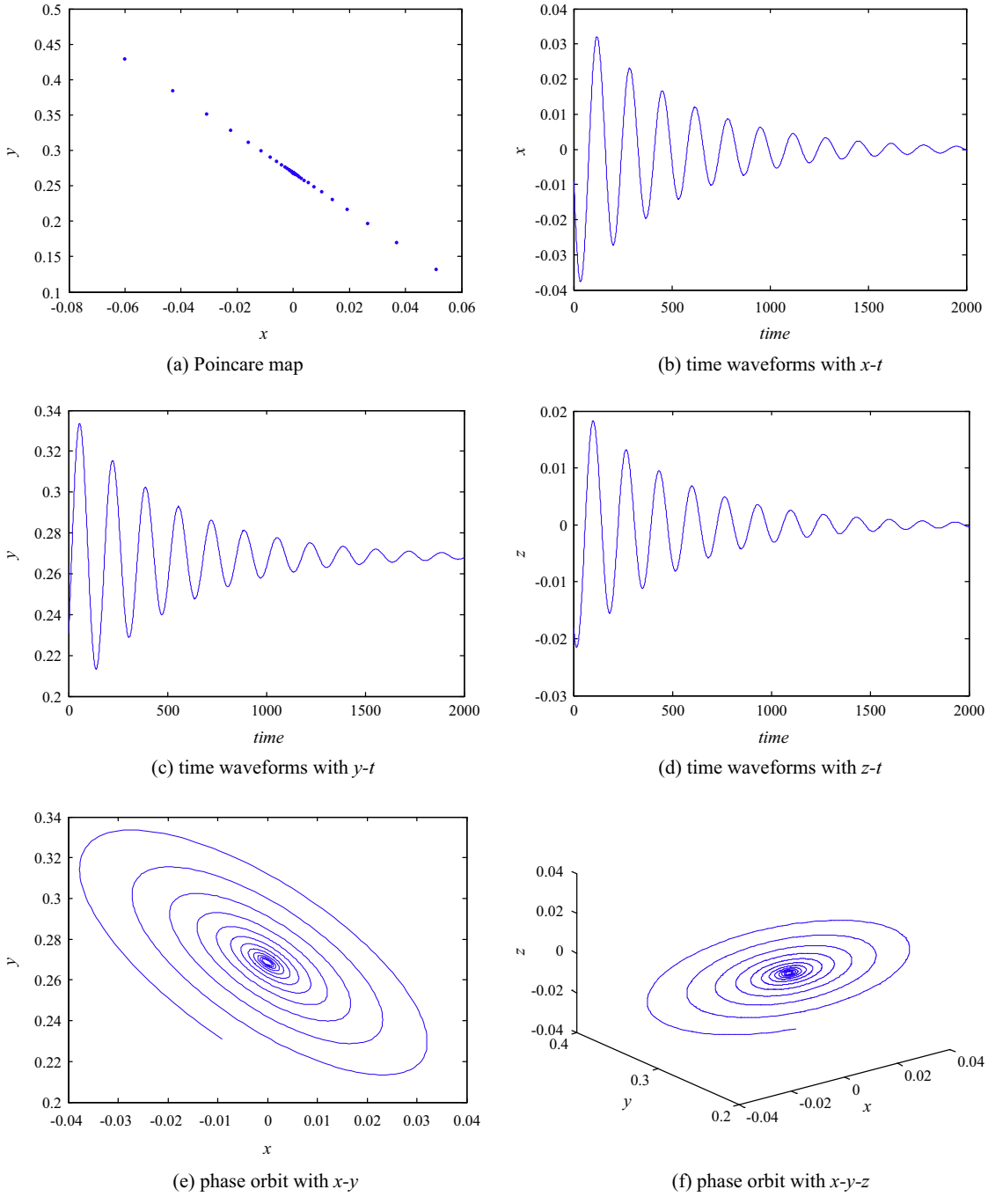

(a) Poincare map

(b) time waveforms with x-t

(c) time waveforms with y-t

(d) time waveforms with z-t

(e) phase orbit with x-y

(f) phase orbit with x-y-z

Fig. 7. Poincare maps, time waveforms and phase orbits with $t = 2.5$.

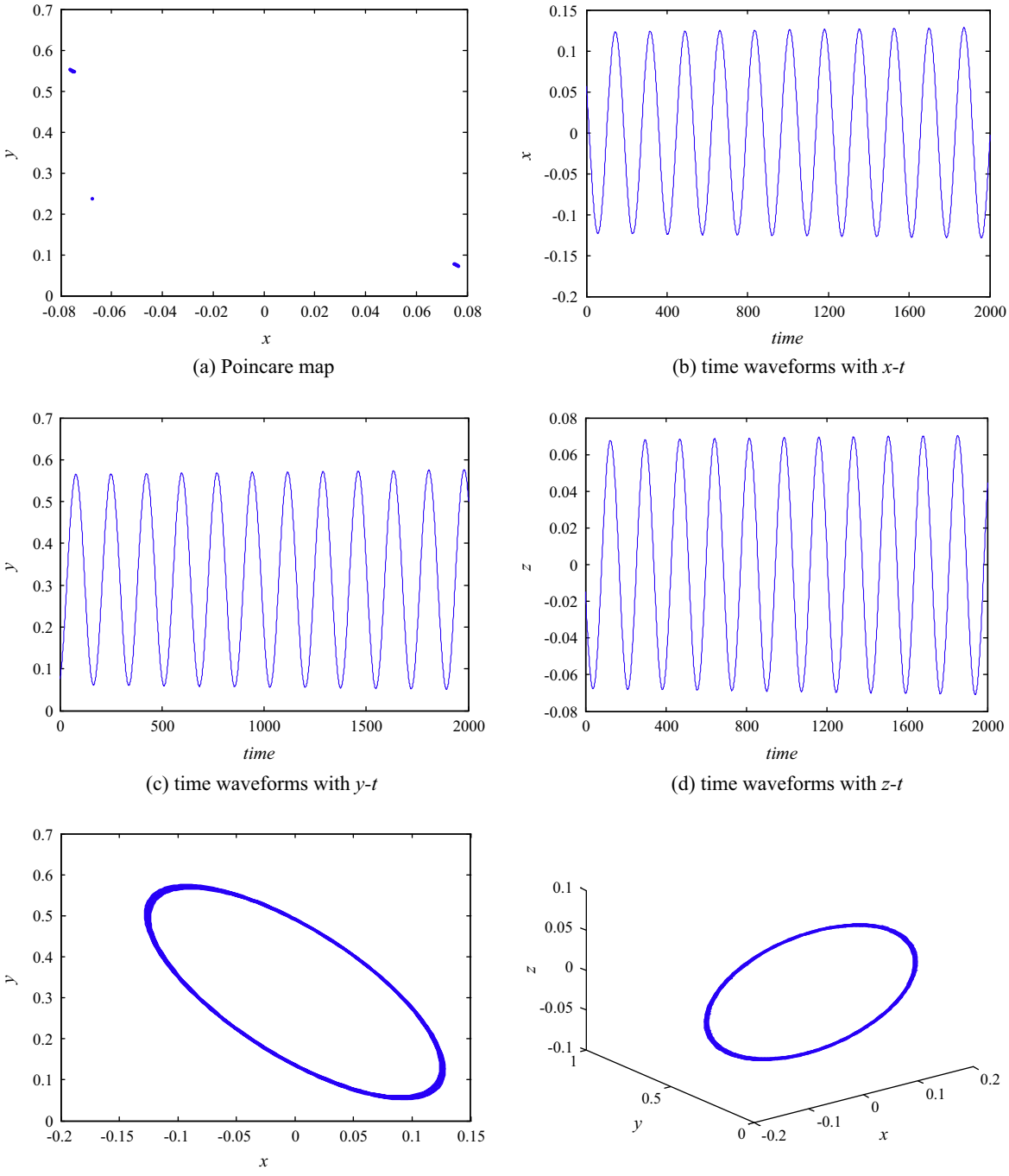

(a) Poincare map (b) time waveforms with *x-t*

(c) time waveforms with *y-t* (d) time waveforms with *z-t*

(e) phase orbit with *x-y* (f) phase orbit with *x-y-z*

Fig. 8. Poincare maps, time waveforms and phase orbits with $t = 2.63$.

2.6. Nonlinear model of governing system in the process of load rejection transient

Considering the nonlinear transfer coefficients, the nonlinear expressions between transfer coefficients and time t is presented. And to some extent, the nonlinear dynamic model is set up to reflect the essence of nonlinear system.

Supposing the water diversion system is the rigid water-hammer model, and the hydro-turbine control system is under PID control.

Through above analysis, nonlinear dynamic model of governing system in the process of load rejection transient can be obtained as

$$\begin{cases} \dot{x} = -\frac{(2e_{mw}-e_g)}{T_{ab}}x + \frac{e_{my}}{T_{ab}}y + \frac{e_{mh}}{T_{ab}}h - \frac{1}{T_{ab}}m_{g0} \\ \dot{y} = \frac{1}{T_y}[k_p(r-x) + k_i z - k_d\dot{x} - y] \\ \dot{h} = \frac{1}{e_{qh}}\left\{\frac{(e_g-e_{mw})e_{qw}}{T_{ab}}x + \left[\frac{e_{qy}}{T_y} - \frac{e_{qw}e_{my}}{T_{ab}}\right]y - \left(\frac{e_{qw}e_{mh}}{T_{ab}} + \frac{1}{T_w}\right)h - \frac{e_{qy}}{T_y}[k_p(r-x) \right. \\ \qquad \left. + k_i z - k_d\dot{x}] + \frac{e_{qw}}{T_{ab}}m_{g0}\right\} \\ \dot{z} = r - x \end{cases} \tag{24}$$

Substituting Eqs. (18)–(23) into Eq. (24), the nonlinear dynamic model of governing system can be got as

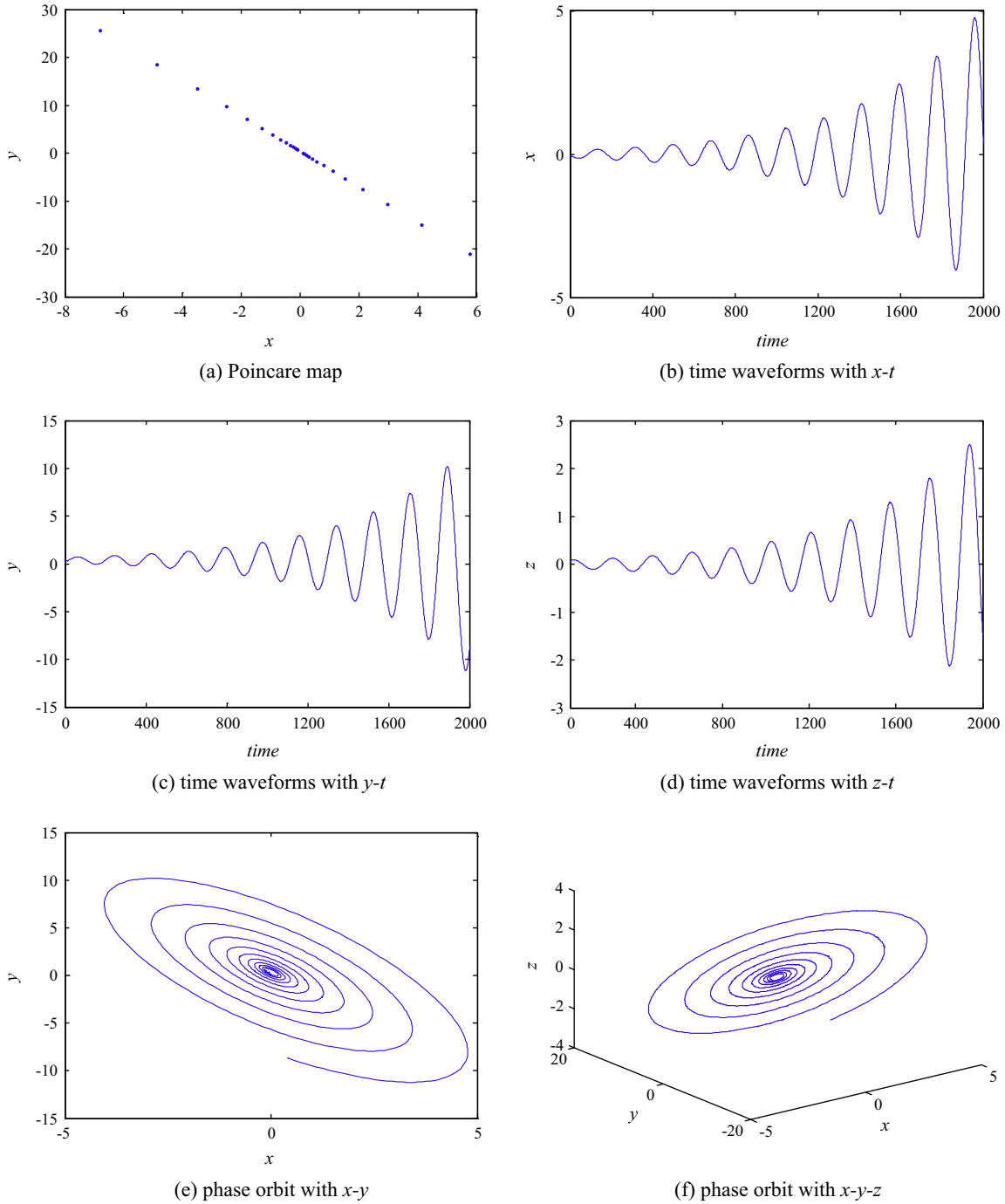

(a) Poincare map (b) time waveforms with *x-t*

(c) time waveforms with *y-t* (d) time waveforms with *z-t*

(e) phase orbit with *x-y* (f) phase orbit with *x-y-z*

Fig. 9. Poincare maps, time waveforms and phase orbits with $t = 2.8$.

$$
\begin{cases}
\dot{x} = -\frac{\left(\cos\left(\frac{2}{3}\pi t+\pi\right)-1-e_g\right)}{T_{ab}}x + \frac{\left(\cos\left(\frac{2}{3}\pi t+\pi\right)+2\right)}{T_{ab}}y + \frac{\left(\cos\left(\frac{2}{3}\pi t+\frac{1}{3}\pi\right)+1\right)}{T_{ab}}h - \frac{1}{T_{ab}}m_{g0} \\
\dot{y} = \frac{1}{T_y}[k_p(r-x) + k_i z - k_d\dot{x} - y] \\
\dot{h} = \frac{1}{\frac{1}{4}\sin\left(\frac{2}{3}\pi t+\pi\right)+\frac{1}{2}}\left\{\frac{\left(e_g-\left(\frac{1}{2}\cos\left(\frac{2}{3}\pi t+\pi\right)-\frac{1}{2}\right)\right)\cdot\left(\frac{1}{10}\sin\left(\frac{2}{3}\pi t-\frac{\pi}{2}\right)-\frac{1}{10}\right)}{T_{ab}}x\right. \\
\quad + \left[\frac{\frac{1}{2}\sin\left(\frac{2}{3}\pi t-\frac{1}{2}\pi\right)+\frac{3}{2}}{T_y} - \frac{\left(\frac{1}{10}\sin\left(\frac{2}{3}\pi t-\frac{\pi}{2}\right)-\frac{1}{10}\right)\cdot\left(\cos\left(\frac{2}{3}\pi t+\pi\right)+2\right)}{T_{ab}}\right]y \\
\quad - \left(\frac{\left(\frac{1}{10}\sin\left(\frac{2}{3}\pi t-\frac{\pi}{2}\right)-\frac{1}{10}\right)\cdot\left(\cos\left(\frac{2}{3}\pi t+\frac{1}{3}\pi\right)+1\right)}{T_{ab}} + \frac{1}{T_w}\right)h \\
\quad \left. - \frac{\frac{1}{2}\sin\left(\frac{2}{3}\pi t-\frac{1}{2}\pi\right)+\frac{3}{2}}{T_y}[k_p(r-x) + k_i z - k_d\dot{x}] + \frac{\frac{1}{10}\sin\left(\frac{2}{3}\pi t-\frac{\pi}{2}\right)-\frac{1}{10}}{T_{ab}}m_{g0}\right\} \\
\dot{z} = r - x
\end{cases}
\tag{25}
$$

3. Nonlinear dynamic analyses

A new kind of control method is proposed, which keeps the PID parameters invariant in the process of load rejection transient. The numerical simulation results are carried out by using the method of Runge–Kutta. More specially, the fixed step is $\frac{2\pi}{125}$, the initial values are (0.0001, 0.0001, 0, 0), the iteration steps are 2000.

System parameters are as follows

$$T_y = 0.2,\ T_{ab} = 5.5,\ T_w = 2,\ r = 0,\ m_{g0} = 0.4.$$

PID adjustor parameters are as follows

$$k_p = 1.6,\ k_i = 1.2,\ k_d = 3.$$

The bifurcation diagram of turbine speed about time t is shown in Fig. 4(a). Fig. 4(b) and (c) are the magnification of turbine speed for the time range of 0.2–0.4 and 2.5–3, respectively.

The results of the numerical simulation are illustrated by bifurcation diagrams, Poincare maps, time waveforms and dynamical orbits. First, for the sake of having an overview of the essential dynamics of the governing system, the bifurcation diagram about t is presented as shown in Fig. 4. From the local amplification of bifurcation diagram, we can know that there are two important points ($t = 0.22$ and $t = 2.63$), for the range $0.22 < t < 2.63$, the system is obviously steady. Second, in order to further study the dynamical behaviors, Poincare maps, time waveforms and phase orbits are presented with different t.

For $t = 0.1$, as shown in Fig. 5, the turbine speed, the deviation of wicket gate position and turbine head increase gradually, and linear distribution of the points appear in the Poincare map. Therefore, we know that the governing system tend to be unstable.

Fig. 6 shows Poincare map, time waveforms and phase orbits with $t = 0.22$. The motion regularities of the turbine speed, the deviation of wicket gate position and turbine head are periodical. A limit cycle appeared in the phase orbit. And only two points turn up in the Poincare map. All of these results indicate that the governing system makes a periodic vibration and further reveal that the system cannot tend to be stable.

The system dynamical behaviors at $t = 2.5$ are shown in Fig. 7. The turbine speed, deviation of wicket gate position and turbine head tend to be a constant. Furthermore, there are some linear points in the Poincare map. A regular circle appeared in the phase orbit. Therefore, all these results indicate that the system can better cope with disturbances and keep steady at this value of the differential adjustment coefficient.

The responses of the governing system with $t = 2.63$ are respectively illustrated in Fig. 8 using Poincare map, time waveforms and phase orbit. From Fig. 8 the turbine speed, deviation of wicket gate position and turbine head tend to be periodic motion. Furthermore, there are only some isolated points in the Poincare map. These results indicate that the governing system is in the critical state at this time.

The Poincare map, time waveforms and phase orbit of the unstable responses of system with $t = 2.8$ are shown in Fig. 9. The turbine speed, deviation of wicket gate position and turbine head has left their original position gradually, which indicate that the governing system would lose stability finally.

4. Conclusions

Firstly, a nonlinear dynamic mathematical model of governing system in the process of load rejection transient is proposed using the nonlinear dynamic transfer coefficients. Secondly, the nonlinear dynamical behaviors of the governing system are presented including bifurcation diagrams, time waveforms, phase orbits and Poincare maps. The numerical simulation results indicate that the governing system is steady in the range of $0.22 < t < 2.63$ and the two important points ($t = 0.22$ and $t = 2.63$) are the critical points of the governing system in the process of load rejection transient. This paper can provide a basis for the further study of dynamic behaviors and systematic control methods of hydro-turbine governing system in the process of load rejection transient.

Acknowledgements

This wok was supported by the scientific research foundation of National Natural Science Foundation (51109180 and 51479173), the National Science & Technology Supporting Plan from the Ministry of Science & Technology of PR China (2011BAD29B08), the Fundamental Research Funds for the Central Universities of Ministry of Education of China (201304030577), Northwest A&F University Foundation, China (2013BSJJ095) and the Scientific Research Foundation of National Natural Science Foundation (51279167).

References

[1] Chen ZH, Yuan XH, Tian H, Ji B. Improved gravitational search algorithm for parameter identification of water turbine regulation. Energy Convers Manage 2014;78:306–15.
[2] Moradi H, Alasty A, Vossoughi G. Nonlinear dynamics and control of bifurcation to regulate the performance of a boiler-turbine unit. Energy Convers Manage 2013;68:105–13.
[3] Pico HV, McCalley JD, Angel A, Leon R, Castrillon NJ. Analysis of very low frequency oscillations in hydro-dominant power systems using multi-unit modeling. IEEE Trans Power Syst 2012;27:1906–15.
[4] Wang W, Zeng DL, Liu JZ, Niu YG, Cui C. Feasibility analysis of changing turbine load in power plants using continuous condenser pressure adjustment. Energy 2014;64:533–40.
[5] Zeng Y, Zhang LX, Guo YK, Qian J, Zhang CL. The generalized Hamiltonian model for the shafting transient analysis of the hydro turbine generating sets. Nonlinear Dyn 2014;76:1921–33.
[6] Karimi M, Mohamad H, Mokhlis H, Bakar AHA. Under-frequency load shedding scheme for islanded distribution network connected with mini-hydro. Int J Electr Power Energy Syst 2012;42:127–38.
[7] Li CS, Zhou JZ. Parameters identification of hydraulic turbine governing system using improved gravitational search algorithm. Energy Convers Manage 2011;52:374–81.
[8] Nagode K, Skrjanc I. Modelling and internal fuzzy model power control of a Francis water turbine. Energies 2014;7:874–89.
[9] Ling DJ, Tao Y. An analysis of the Hopf bifurcation in a hydroturbine governing system with saturation. IEEE Trans Energy Convers 2006;21:512–5.
[10] Ren MF, Wu D, Zhang JH, Jiang M. Minimum entropy-based cascade control for governing hydroelectric turbines. Entropy 2014;16:3136–48.
[11] Michelsen FA, Wihelmsen O, Zhao L, Asen KI. A distributed dynamic model of a monolith hydrogen membrane reactor. Energy Convers Manage 2013;67:160–70.
[12] Date A, Date A, Akbarzadeh A. Investigating the potential for using a simple water reaction turbine for power production from low head hydro resources. Energy Convers Manage 2013;66:257–70.
[13] Kishor N, Saini RP, Singh SP. A review on hydropower plant models and control. Renew Sust Energy Rev 2007;11:776–96.
[14] Williamson SJ, Stark BH, Booker JD. Low head pico hydro turbine selection using a multi-criteria analysis. Renew Energy 2014;61:43–50.
[15] Fang HQ, Chen L, Shen ZY. Application of an improved PSO algorithm to optimal tuning of PID gains for water turbine governor. Energy Convers Manage 2011;52:1763–70.
[16] Das S, Pan I, Das S. Fractional order fuzzy control of nuclear reactor power with thermal-hydraulic effects in the presence of random network induced delay and sensor noise having long range dependence. Energy Convers Manage 2013;68:200–18.
[17] Zhu H, Huang WW, Huang GH. Planning of regional energy systems: an inexact mixed-integer fractional programming model. Appl Energy 2014;113:500–14.
[18] Zhu H, Huang GH. Dynamic stochastic fractional programming for sustainable management of electric power systems. Int J Electr Power Energy Syst 2013;53:553–63.
[19] Ozdemir MT, Sonmez M, Akbal A. Development of FPGA based power flow monitoring system in a microgrid. Int J Hydrogen Energy 2014;39:8596–603.
[20] Chilipi RR, Singh B, Murthy SS, Madishetti S, Bhuvaneswari G. Design and implementation of dynamic electronic load controller for three-phase self-excited induction generator in remote small-hydro power generation. IET Renew Power Generation 2014;8:269–80.
[21] Chen DY, Ding C, Ma XY, Yuan P, Ba DD. Nonlinear dynamical analysis of hydro-turbine governing system with a surge tank. Appl Math Model 2013;37:7611–23.
[22] Jiang CW, Ma YC, Wang CM. PID controller parameters optimization of hydro-turbine governing systems using deterministic–chaotic-mutation evolutionary programming (DCMEP). Energy Convers Manage 2006;47:1222–30.
[23] Xu Y, Li ZH. Computational model for investigating the influence of unbalanced magnetic pull on the radial vibration of large hydro-turbine generators. J Vib Acoust Trans ASME 2012;134:051013.
[24] Kishor N, Singh SP, Raghuvanshi AS. Dynamic simulations of hydro turbine and its state estimation based LQ control. Energy Convers Manage 2006;47:3119–37.
[25] Zeng Y, Guo YK, Zhang LX, Xu TM, Dong HK. Nonlinear hydro turbine model having a surge tank. Math Comput Model Dyn Syst 2013;19:12–28.
[26] Fang HQ, Chen L, Dlakavu N, Shen ZY. Basic modeling and simulation tool for analysis of hydraulic transients in hydroelectric power plants. IEEE Trans Energy Convers 2008;23:834–41.
[27] Chen ZH, Yuan XH, Ji B, Wang PT, Tian H. Design of a fractional order PID controller for hydraulic turbine regulating system using chaotic non-dominated sorting genetic algorithm II. Energy Convers Manage 2014;84:390–404.

[28] Chen DY, Ding C, Do YH, Ma XY, Zhao H, Wang YC. Nonlinear dynamic analysis for a Francis hydro-turbine governing system and its control. J Franklin Inst – Eng Appl Math 2014;351:4596–618.
[29] Chen ZH, Yuan XH, Tian H, Ji B. Improved gravitational search algorithm for parameter identification of water turbine regulation system. Energy Convers Manage 2014;78:306–15.
[30] Shen ZY. Hydraulic turbine regulation. Beijing: China WaterPower Press; 1998 [in Chinese].
[31] Shou MH, Zhang XB. Study on the dynamic model of the hydro-turbine linear control system. J Electr Eng 1984;4:48–57 [in Chinese].
[32] IEEE Working Group. Hydraulic-turbine and turbine control-models for system dynamic studies. IEEE Trans Power Syst 1992;7:167–79.
[33] Smith JR. Assessment of hydraulic models for power-system studies. IEE Proc C 1983;130:1–7.